

The Internal Kinematics, Stellar Population, and Gas-phase Properties of The Pseudobulge in An Ultra-diffuse Galaxy: AGC721966

SHIHONG LIU,^{1,2} YU RONG*,^{1,2} HUIYUAN WANG,^{1,2} HONG-XIN ZHANG,^{1,2} TIE LI,^{1,2} YAO YAO,^{1,2} ZHICHENG HE,^{1,2} TENG LIU,^{1,2}
 ENCI WANG,^{1,2} CHENG CHENG,³ AND XU KONG^{1,2}

¹*Department of Astronomy, University of Science and Technology of China, Hefei, Anhui 230026, China*

²*School of Astronomy and Space Sciences, University of Science and Technology of China, Hefei 230026, Anhui, China*

³*National Astronomical Observatories, Chinese Academy of Sciences, Beijing 100012, China*

ABSTRACT

Leveraging spectroscopic data from the Sloan Digital Sky Survey, we conduct a comprehensive analysis of the central stellar velocity dispersion, stellar population properties, star formation history, and gas-phase chemical abundances in AGC721966, a unique ultra-diffuse galaxy (UDG) harboring a pseudobulge. Our findings reveal that the pseudobulge formed in the early universe but underwent a recent episode of rejuvenated star formation. The system exhibits a mass-weighted (light-weighted) stellar population age of $\tau_* \sim 7.4 \pm 2.5$ (2.9 ± 1.5) Gyr, a stellar metallicity of $[\text{M}/\text{H}] \sim -0.62 \pm 0.26$ (-0.55 ± 0.20), an α -element enhancement of $[\alpha/\text{Fe}] \sim 0.36 \pm 0.09$ (0.37 ± 0.07), and a gas-phase oxygen abundance of $12 + \log(\text{O/H}) \sim 8.15 \pm 0.03$. The central stellar velocity dispersion is measured as $\sigma_c \sim 57.9 \pm 15.7$ km/s. These results provide robust evidence supporting the early halo-halo merging formation scenario proposed by Rong et al. (2025), while unequivocally ruling out the “failed” L^* formation model, at least for AGC721966. Furthermore, through systematic application of the baryonic Tully-Fisher relation, we establish that these pseudobulge-hosting UDGs are neither misidentified nuclear star cluster-bearing dwarf galaxies nor bulge-dominated massive galaxies, thereby affirming their distinct evolutionary pathway.

Keywords: galaxies: dwarf — galaxies: spectroscopy — galaxies: evolution

1. INTRODUCTION

Ultra-diffuse galaxies (UDG; van Dokkum et al. 2015) are characterized by effective radii comparable to the Milky Way yet stellar masses akin to dwarf galaxies. Early observations of UDGs in galaxy clusters suggested a high dark matter fraction, inferred from their resilience to tidal disruption, which posited that diffuse stellar distributions might be shielded by massive dark matter halos. The detection of a putative $10^{12} M_\odot$ (van Dokkum et al. 2016) halo in the Coma UDG, DF44, initially bolstered this hypothesis (van Dokkum et al. 2016), prompting speculation that UDGs represent “failed L^* galaxies” (FLGs; van Dokkum et al. 2015)—systems stunted in star formation efficiency by early environmental effects or internal feedback (Yozin et al. 2015). However, subsequent studies leveraging weak lensing, globular cluster counts, and X-ray data revealed that most UDGs reside in dwarf-scale halos (Sifón et al. 2018; Amorisco et al. 2018; Marleau et al. 2024; Kovács et al. 2019), though a subset with abundant globular clusters may still align with FLG scenarios (Lim et al. 2020; Gannon et al. 2022).

Corresponding author: Yu Rong
 rongyua@ustc.edu.cn

A paradigm shift occurred with the discovery of UDGs DF2 and DF4 van Dokkum et al. (2018, 2019), which exhibit negligible dark matter content. These findings challenge empirical galaxy evolution models, which predict halo masses of $10^{10} - 10^{11} M_\odot$ for galaxies with UDG-like stellar masses ($10^7 - 10^9 M_\odot$). Such discrepancies—whether excess or deficit—underscore that UDG formation mechanisms may fundamentally diverge from canonical pathways.

Numerous models attempt to reconcile these observations. High-spin halos (Rong et al. 2017; Amorisco & Loeb 2016; Liao et al. 2019; Benavides et al. 2023; Rong et al. 2024a, 2020) and supernova-driven outflows (Di Cintio et al. 2016; Chan et al. 2018; Cardona-Barrero et al. 2020) reproduce UDG scaling relations but struggle with overproduction or structural inconsistencies. Alternative frameworks invoke dwarf mergers (Wright et al. 2021), tidal heating (Carleton et al. 2019; Jiang et al. 2019), ram-pressure stripping (Grishin et al. 2021), or self-interacting dark matter (Zhang et al. 2025).

Recent observations of field UDGs with pseudobulges (Rong et al. 2025)—unprecedented in dwarf galaxies (Kormendy et al. 2010; Kormendy & Bender 2012)—offer a new avenue to probe their origins. These systems host extended, rotationally supported disks alongside pseudobulges (Sérsic index $n < 2.5$, stellar mass $M_* \sim 10^{8.0} - 10^{8.7} M_\odot$, and effective radius $r_h \sim 300 - 700$ pc), far exceeding nuclear

star cluster dimensions (Walcher et al. 2006; Georgiev et al. 2016; Spengler et al. 2017; Neumayer & Seth 2020; Hilker et al. 1999; Drinkwater et al. 2000). Their elevated HI-derived rotation velocities and pseudobulge presence suggest halo masses exceeding typical dwarfs, potentially bridging UDGs to FLGs or early gas-rich mergers (Bekki 2008).

Resolving whether these UDGs harbor supermassive black holes (SMBHs) or originate from halo mergers requires empirical validation of their star formation histories (SFHs), stellar kinematics, and halo masses. Here, we present spectroscopic analysis of the pseudobulge-hosting UDG AGC721966, quantifying its central velocity dispersion, stellar population parameters, and gas-phase abundances. By coupling these results with dynamical mass estimates and baryonic Tully-Fisher constraints, we probe the system’s formation pathway and dark matter content. The paper is structured as follows: Section 2 details spectral fitting techniques and derives the central velocity, stellar population, gas-phase chemical abundance; Section 3 interprets the derived black hole mass and halo mass, evaluates formation scenarios, and recalibrates distances via baryonic Tully-Fisher relations. Conclusions are synthesized in Section 4. Throughout this paper, “log” represents “ \log_{10} ”.

2. SPECTROSCOPY FOR THE PSEUDOBULGE OF AGC721966

Among the five pseudobulge-hosting UDGs identified by Rong et al. (2025), AGC721966 stands out as the nearest system, with a distance of 78.9 ± 2.3 Mpc. Spectroscopic data for this galaxy were obtained from the Sloan Digital Sky Survey (SDSS; Data Release 12 (DR12), Alam et al. 2015), targeting its central region through a 3''-diameter fiber aperture, as shown by the insert of panel a in Fig. 1. At the distance of AGC721966, this aperture corresponds to a physical scale of approximately 1.1 kpc, fully encompassing the pseudobulge (effective radii $r_h \sim 0.4$ kpc in g -band and 0.60 kpc in r -band, respectively). The central surface brightness of the pseudobulge in the g -band ($\mu_g \sim 16$ mag/arcsec 2) starkly contrasts with that of the surrounding disk ($\mu_g \sim 25$ mag/arcsec 2), indicating that the disk contributes negligibly to the central luminosity (< 0.1% of the total flux within the fiber). Consequently, the SDSS spectrum predominantly reflects the pseudobulge’s properties, with negligible contamination from the disk.

The spectrum exhibits a signal-to-noise ratio (S/N) of ~ 25 (measured across 5450–5550 Å), sufficient for robust stellar dynamical and population synthesis analyses following spectral rebinning. Prior to analysis, the spectrum was corrected for Galactic extinction using the Fitzpatrick (1999) extinction law with $R_V = 3.1$ and $E(B-V)$ values retrieved from the NASA/IPAC Extragalactic Database (NED).

2.1. Stellar velocity dispersion

Building upon the methodology of Rong et al. (2020), we employ the penalized pixel-fitting code PPXF (v7.3.0; Cappellari 2017) to perform spectral fitting and derive the central stellar velocity dispersion σ_c of the pseudobulge in

AGC721966. Our implementation adopts 6th-order additive (“degree”) and multiplicative (“mdegree”) polynomials, a configuration optimized to mitigate template mismatch and continuum variations (Emsellem et al. 2004; Guérou et al. 2017; Spinello et al. 2021; Bidaran et al. 2020).

To maximize dispersion measurement fidelity, we utilize the Indo-US stellar template library (Valdes et al. 2004), selected for its high spectral resolution (FWHM=1.35 Å; Beifiori et al. 2011), and mask all emission-line regions during the fitting process. Following instrumental resolution correction (SDSS spectrum FWHM=2.76 Å, corresponding to a velocity resolution of ~ 64 km/s at 5500 Å), we measure $\sigma_c \simeq 57.9 \pm 15.7$ km/s for the pseudobulge, where uncertainties are derived via bootstrap resampling as per Fahrion et al. (2025); Kacharov et al. (2018). This dispersion substantially exceeds values characteristic of nuclear star clusters (NSC; $\sigma_{\text{NSC}} \sim 10 - 40$ km/s) and globular cluster (GC; $\sigma_{\text{GC}} \sim 3 - 25$ km/s) observed in UDGs (e.g., Fahrion et al. 2025; Khim et al. 2025) and dwarf galaxies (e.g., Neumayer & Seth 2020; Nguyen et al. 2017; Seth et al. 2008).

Robustness tests confirm that σ_c remains within the 1σ uncertainty range when varying polynomial orders (“degree”=4, 5, 7, 8, 10; “mdegree”=5, 8, 10, 12), demonstrating insensitivity to fitting polynomials choices.

2.2. Stellar population and SFH

To conduct stellar population synthesis (SPS), we employ the MILES single stellar population (SSP) spectral templates (Vazdekis et al. 2015), circumventing the absence of age information in the Indo-US library. Although MILES exhibits lower spectral resolution (FWHM= 2.5 Å), compared to Indo-US, its comprehensive age-metallicity parameter space renders it optimal for SPS.

Our analysis leverages MILES models calibrated using BaSTI isochrones (Pietrinferni et al. 2006) and a bimodal Milky Way-like initial mass function (IMF) with a high-mass slope of 1.30. The grid spans 53 ages (from 30 Myr to 14 Gyr) and 12 metallicities (from [M/H]=-0.27 to +0.40). Given the MILES library’s restriction to scaled-solar ([α /Fe]=0) and α -enhanced ([α /Fe]=0.4 dex) templates, we adopt the methodology of Fahrion et al. (2019) to construct a finely sampled SSP grid. We systematically interpolate between existing templates at 0.1 dex intervals across [α /Fe]=0.0 to [α /Fe]=0.4 dex, with extrapolation to [α /Fe]=-0.1 dex, assuming linear α -abundance behavior within this regime. This α -variable grid enables robust recovery of average [α /Fe] from spectral features.

During the fitting process, we rebin the spectrum by combining every two adjacent data points into a single point to enhance the spectrum SNR. After binning, the spectrum SNR increases to ~ 33 . We disable additive polynomials and regularization (“REG_ORD”=0) in PPXF to minimize overfitting. The rebinned spectrum and best-fit stellar model are shown in panel a of Fig. 1. The resulting mass-weighted parameters are total-metallicity [M/H]= -0.62 ± 0.26 , stellar age $\tau_* = 7.4 \pm 2.5$ Gyr, and $[\alpha/\text{Fe}] \simeq 0.36 \pm 0.09$; light-weighted values are [M/H]~ -0.55 ± 0.20 , $\tau_* \sim$

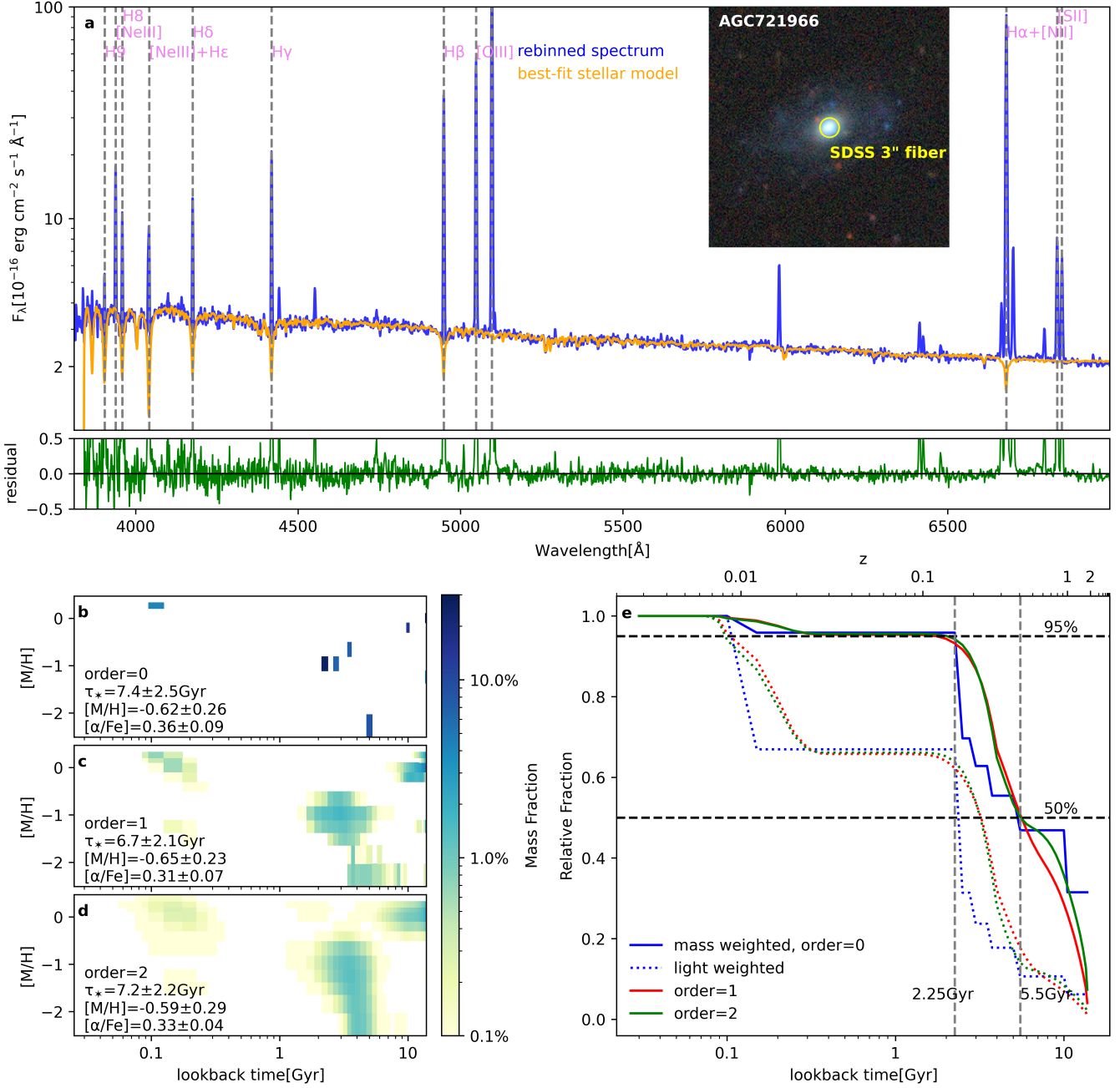


Figure 1. Stellar population analysis of the pseudobulge in AGC721966. Panel a presents the SDSS spectrum of the pseudobulge after rebinning (blue), best-fit stellar population model (orange), and residuals (green). The inset displays the image of AGC721966, highlighting the SDSS 3 arcsec spectroscopic fiber positioned on the pseudobulge of the galaxy. Panels b, c, and d show the mass-weighted stellar age-metallicity distributions, illustrating the SFH derived without regularization (b), with first-order regularization (c), and with second-order regularization (d). The color bar indicates the mass fractions corresponding to each combination of age and metallicity. Panel e: mass assembly (solid lines) and light assembly (dotted lines) of the pseudobulge, with results shown for the unregularized case (blue), first-order regularization (red), and second-order regularization (green). The horizontal black dashed lines mark the epochs when 50% and 95% of the stellar mass or light had been assembled, respectively.

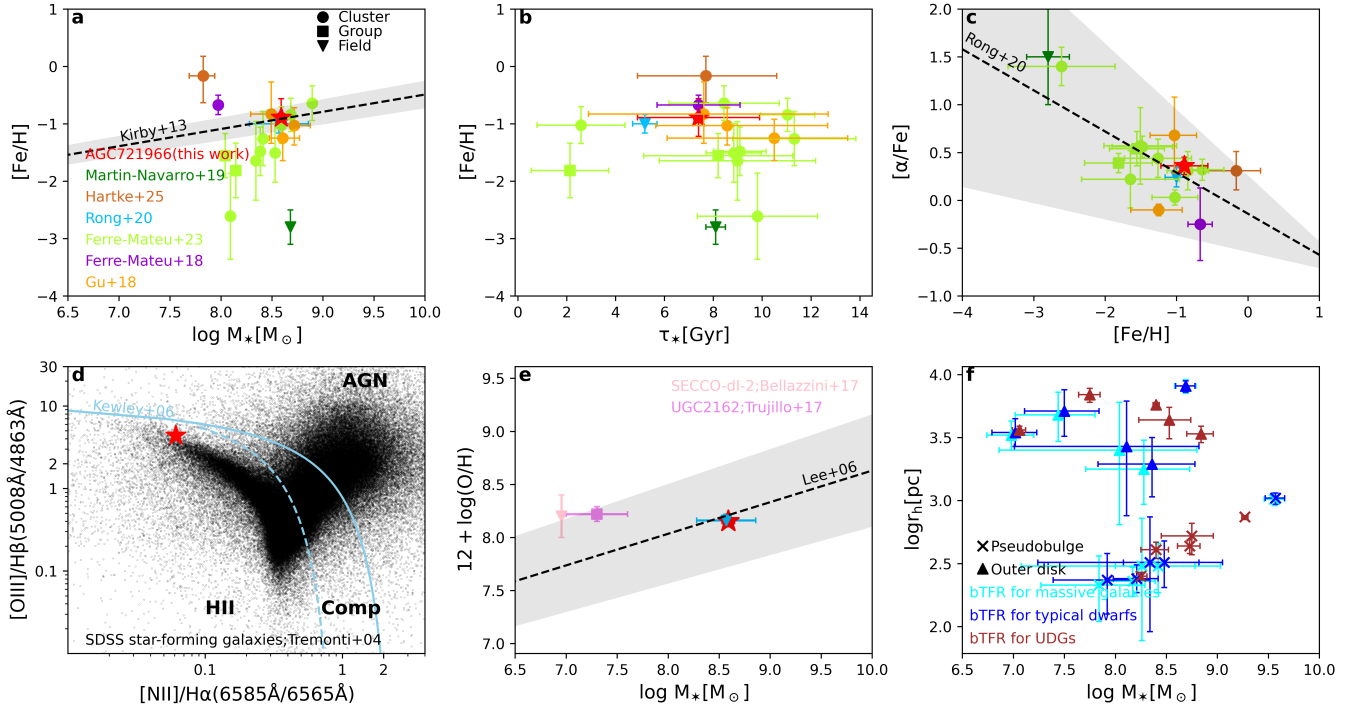


Figure 2. Comparative analysis of the pseudobulge in AGC721966 and other UDGs. Symbols denote UDGs in different environments: dots for galaxy clusters, squares for groups, and inverted triangles for field galaxies. The pseudobulge in AGC721966 is highlighted as a red star. Panel a: the mass-weighted stellar metallicity $[Fe/H]$ as a function of stellar mass M_* . The universal $[Fe/H]-M_*$ relation for nearby dwarf galaxies (Kirby et al. 2013) is shown as a black dashed line, with its 1σ uncertainty represented by the grey shaded region. Panel b: $[Fe/H]$ versus mass-weighted stellar ages τ_* . Panel c: α -element enhancement as a function of $[Fe/H]$. The $[\alpha/Fe]-[Fe/H]$ relation for typical UDGs (Rong et al. 2020) is indicated by a dashed line, with the 1σ uncertainty region shaded in grey. Note that the results shown in panel a to c are all mass-weighted. Panel d: $12+\log(O/H)$ versus M_* , with the mass-metallicity relation for nearby star-forming dwarfs (Lee et al. 2006) overlaid as a dashed line and its 1σ uncertainty as a grey region. Panel e: BPT diagram showing SDSS star-forming galaxies (small black dots) and the pseudobulge in AGC721966. The curves for AGN selection (Kewley et al. 2006) are also displayed. Panel f: size-mass relations for pseudobulges (crosses) and outer stellar disks (triangles) of five UDGs hosting pseudobulges (Rong et al. 2025), using distances derived from the bTFR. The cyan, blue, and magenta colors correspond to the application of typical bTFRs for gas-dominant massive galaxies (Stark et al. 2009), typical dwarf galaxies (Lelli et al. 2016), and gas-rich UDGs (Rong et al. 2024a), respectively.

2.9 ± 1.5 Gyr, and $[\alpha/\text{Fe}] \sim 0.37 \pm 0.07$. Iron abundance is derived as $[\text{Fe}/\text{H}] = [\text{M}/\text{H}] - 0.75[\alpha/\text{Fe}]$ (Vazdekis et al. 2015).

Figure 1 compares SSP solutions under first- and second-order regularization. While regularization smoothes age-metallicity template weights—optimal for systems with prolonged star formation—all approaches yield parameters consistent within 1σ uncertainties. Tests with multiplicative polynomial orders (“mdegree”= 5, 8, 10, 12) confirm result stability.

The pseudobulge aligns with the universal $[\text{Fe}/\text{H}] - M_*$ relation of dwarf galaxies (Kirby et al. 2013), as explored in panel a of Fig. 2, yet its age mirrors cluster/group UDGs (Gu et al. 2018; Ferré-Mateu et al. 2018, 2023; Hartke et al. 2025) rather than isolated counterparts (Rong et al. 2020), as indicated in panel b of Fig. 2. Its $[\alpha/\text{Fe}]-[\text{Fe}/\text{H}]$ trend matches typical UDGs across environments (Rong et al. 2020), as shown in panel c of Fig. 2. Our results indicate that the pseudobulge of AGC721966 is indeed old, and plausibly formed by starbursts with short star-formation timescales.

As shown in panel e of Fig. 1, unregularized and regularized SFH reconstructions consistently reveal the early formation of the pseudobulge. Approximately 50% of the stellar mass of the pseudobulge was formed before lookback time $t \sim 5.5$ Gyr, while 95% mass was assembled before $t \sim 2.25$ Gyr. This SFH contrasts with the extended star formation in typical UDGs (Ferré-Mateu et al. 2018; Martín-Navarro et al. 2019; Rong et al. 2020) and single-burst SFH of GCs (Holtzman et al. 1992; O’Connell et al. 1995; Whitmore et al. 1999), instead resembling nuclear star clusters in dwarfs (Johnston et al. 2020; Neumayer & Seth 2020). Yet it does not mean that this galaxy is a nucleated dwarf, as discussed in section 3.4

2.3. Emission line properties

The strong Balmer line emission and a big difference between the mass- and light-weighted ages indicate recent gas accretion and localized star formation rejuvenation.

Following subtraction of the best-fit stellar population model from the stacked spectrum, we perform Gaussian profile fitting to individual emission lines and calculate the $\text{H}\alpha/\text{H}\beta$ flux ratio to estimate dust extinction under Case-B recombination assumptions (Hummer & Storey 1987). The pseudobulge of AGC721966 occupies the star-forming locus in the Baldwin-Phillips-Terlevich (BPT; Baldwin et al. 1981) diagnostic diagram, as explored by panel d of Fig. 2, indicating a low likelihood of active galactic nucleus (AGN) contamination (Kewley et al. 2001, 2006).

To derive the gas-phase oxygen abundance $12+\log(\text{O/H})$, we implement two robust metallicity diagnostics: the N2S2H α index (Dopita et al. 2016) and O3N2 calibration (Pettini et al. 2004). This approach supersedes traditional $[\text{O II}]/[\text{O III}]$ -based methods (Izotov et al. 2006; Kniazev et al. 2004), given the absence of $[\text{O II}]\lambda 3727$ coverage in our spectral window and low SNRs for the $[\text{O II}]\lambda 7320, 7330$ doublet. The N2S2H α diagnostic combines the $[\text{N II}]\lambda 6584/\text{H}\alpha$ and $[\text{N II}]\lambda 6584/[\text{S II}]\lambda 6717, 31$

line ratios, while O3N2 utilizes $[\text{O III}]\lambda 5007/\text{H}\beta$ versus $[\text{N II}]\lambda 6584/\text{H}\alpha$.

Both methods yield consistent oxygen abundances for the pseudobulge: $12+\log(\text{O/H}) \simeq 8.15 \pm 0.02$ (N2S2H α) and $\simeq 8.14 \pm 0.03$ (O3N2). As shown in panel e of Fig. 2, this metallicity aligns with the characteristic $12+\log(\text{O/H}) - M_*$ relation observed in both gas-rich field UDGs (Rong et al. 2020; Trujillo et al. 2017; Bellazzini et al. 2017) and star-forming dwarf galaxies (Lee et al. 2006), reinforcing the pseudobulge’s adherence to canonical chemical evolution pathways.

3. DISCUSSION

3.1. Supermassive black hole?

σ_c provides a basis for estimating central supermassive black hole (SMBH) masses via the well-established $M_{\text{BH}} - \sigma_c$ correlation (Tremaine et al. 2002; Kormendy & Ho 2013; Greene et al. 2016). However, this empirical relation exhibits robust predictive power primarily in elliptical galaxies and systems hosting classical bulges (Häring & Rix 2004; Schutte et al. 2019), while remaining less constrained in pseudobulges. Applying the Tremaine et al. (2002) relation, $M_{\text{BH}} = 10^{8.13 \pm 0.06} M_\odot (\sigma_c/200)^{4.02 \pm 0.32}$, to AGC721966 yields $M_{\text{BH}} \simeq 9.3_{-4.4}^{+6.1} \times 10^5 M_\odot$, placing it near the lower mass boundary of SMBHs ($M_{\text{BH}} \gtrsim 10^6 M_\odot$). Given that pseudobulges typically host black hole masses lower by an order of magnitude compared to classical bulges (Kormendy & Ho 2013; Hu et al. 2008), our results suggest AGC721966 may lack an SMBH, instead potentially harboring an intermediate-mass black hole (IMBH).

Notably, the measured $\sigma_c \sim 57.9$ km/s in AGC721966 exceeds the central velocity dispersions of field UDGs ($\sigma_* \sim 35$ km/s; Rong et al. 2020) by 65%. This disparity implies that, while still inconsistent with SMBH occupation, the putative IMBH in this system may represent a distinct outlier relative to typical UDGs in similar environments, underscoring the potential presence of rare evolutionary pathways or atypical formation conditions.

3.2. Massive halo mass?

The inferred IMBH in AGC721966 implies a relatively low-mass dark matter halo. Aligning with the empirical stellar-to-halo mass relation ($M_* - M_{200}$; Girelli et al. 2020), we estimate a halo mass of $\log M_{200} \simeq 10.70 \pm 0.04$. To independently validate this prediction, we apply an HI kinematics-based approach following Zhang et al. (2025) and Rong et al. (2024a), which circumvents assumptions inherent to $M_* - M_{200}$ or $M_{\text{BH}} - M_{200}$ scaling relations.

First, we derive the dynamical mass enclosed within the HI radius r_{HI} , defined as the radius at which the HI surface density attains $1 M_\odot \text{pc}^{-2}$, as

$$M_{\text{dyn}}(< r_{\text{HI}}) = V_c^2 r_{\text{HI}} / G, \quad (1)$$

where G is the gravitational constant. V_c is the rotation velocity (Rong et al. 2025). The HI radius is determined via the empirically calibrated relation $\log_{10} r_{\text{HI}} = 0.51 \log_{10} M_{\text{HI}} -$

3.59 (Wang et al. 2016; Gault et al. 2021), validated for UDGs (Gault et al. 2021).

Second, assuming a Burkert dark matter profile (Burkert 1995), we compute the halo mass (M_{200}) by solving

$$\begin{aligned} M_{\text{dyn}}(< r_{\text{HI}}) - M_{\text{bar}} &= \int_0^{r_{\text{HI}}} 4\pi r^2 \rho_B(r) dr \\ &= 2\pi\rho_0 r_0^3 \left[\ln \left(1 + \frac{r_{\text{HI}}}{r_0} \right) + 0.5 \ln \left(1 + \frac{r_{\text{HI}}^2}{r_0^2} \right) - \arctan \left(\frac{r_{\text{HI}}}{r_0} \right) \right], \end{aligned} \quad (2)$$

and

$$\begin{aligned} M_{200} &= \int_0^{R_{200}} 4\pi r^2 \rho_B(r) dr \\ &= 2\pi\rho_0 r_0^3 \left[\ln \left(1 + \frac{R_{200}}{r_0} \right) + 0.5 \ln \left(1 + \frac{R_{200}^2}{r_0^2} \right) - \arctan \left(\frac{R_{200}}{r_0} \right) \right] \end{aligned} \quad (3)$$

where $M_{\text{bar}} \simeq M_* + 1.33M_{\text{HI}}$ represents the baryonic mass. M_{HI} is the HI mass. R_{200} represents the virial radius enclosing a mean density that is 200 times the critical value. The core parameters r_0 and ρ_0 are linked via $\log[(r_0/\text{kpc})] = 0.66 - 0.58(\log[M_{200}/10^{11}\text{M}_\odot])$ (Salucci et al. 2007).

Halo mass uncertainties are propagated via Monte Carlo simulations ($N = 1,000$; realizations), incorporating errors in M_{bar} ($\sigma_{M_{\text{bar}}} = \sqrt{\sigma_{M_*}^2 + (1.33\sigma_{M_{\text{HI}}})^2}$), r_{HI} ($\sigma_{r_{\text{HI}}}$), and V_c (σ_{V_c}), and the r_0 - M_{200} relation. The final uncertainty combines the standard deviation of simulated masses with the Burkert profile's intrinsic scatter $\sigma'_{M_{200}} = \sqrt{\sigma_{M_{200}}^2 + (0.15 \text{ dex})^2}$ (Wang et al. 2020).

This yields $\log M_{200} \simeq 11.14 \pm 0.15$, consistent with dwarf-scale halos despite methodological uncertainties (see Zhang et al. 2025, for robustness in HI kinematics for diffuse dwarfs). The HI-derived halo mass exceeds the $M_* - M_{200}$ prediction by 0.44 dex, yet decisively excludes a massive ($\sim 10^{12} \text{ M}_\odot$) dark matter halo for AGC721966.

3.3. Possible formation mechanism?

In our prior investigation of Rong et al. (2025), we proposed two distinct mechanisms to account for the formation of pseudobulge-hosting UDGs, specifically addressing their evolutionary transition from compact bulge-dominated configurations in the early universe to extended disk-like structures at later epochs.

The first posits a “failed L^* ” galaxy scenario, which necessitates a massive dark matter halo ($M_{200} \gtrsim 10^{12} \text{ M}_\odot$) and a central SMBH, to stabilize the system. However, this model conflicts with our observational constraints on AGC721966, which exhibits neither evidence of a massive halo nor SMBH activity. The second mechanism invokes early-universe “star-free” mergers (Rong et al. 2025), wherein gas-rich progenitor halos drive central starbursts to form compact pseudobulges while transferring orbital angular momentum to generate rotationally supported outer disks. Our spectroscopic analysis—revealing an ancient stellar population ($\tau_* \sim 7.4$ Gyr) and pronounced α -element enhancement ($[\alpha/\text{Fe}] \sim 0.36$)—aligns with this merger-driven framework. However, while theoretically viable, this formation model demands rigorous

validation through numerical simulations and spectroscopic studies for more pseudobulges in UDGs.

3.4. Nuclear star cluster?

While the pseudobulge-hosting UDGs identified by Rong et al. (2025) exhibit high radial velocities ($v > 5400 \text{ km/s}$ corresponding to redshift $z > 0.018$), and reside in isolated environments devoid of galaxy groups/clusters, a potential concern still arises: their radial velocities may contain non-negligible peculiar motion components. Such kinematic contamination could artificially inflate distance estimates via Hubble flow assumptions (e.g., Haynes et al. 2018), potentially misclassifying NSCs as pseudobulges due to spatial resolution limitations.

To address this systematically, we employ the baryonic Tully-Fisher relation (bTFR) as an independent distance calibrator. Three distinct bTFR calibrations are applied: (1) the typical bTFR for gas-dominant massive galaxies (Stark et al. 2009), (2) the bTFR for typical dwarf galaxies (Lelli et al. 2016), as well as (3) the bTFR for gas-rich UDGs (Rong et al. 2024a). As demonstrated in panel f of Fig. 2, all three relations robustly confirm the extended nature of these central structures ($r_h > 200 \text{ pc}$)—far exceeding the characteristic sizes of NSCs, UCDs, and GCs which typically have effective radii ranging from approximately 3 pc and 100 pc (Walcher et al. 2006; Georgiev et al. 2016; Spengler et al. 2017; Neumayer & Seth 2020; Hilker et al. 1999; Drinkwater et al. 2000).

Furthermore, the significant ellipticity ($\epsilon = 0.28$ in the r -band) observed in AGC721966’s pseudobulge disfavors NSC interpretations, as nuclear clusters typically exhibit near-circular morphologies, also disfavoring the nuclear star cluster assumption. Collectively, these findings establish that these galaxies, including AGC721966, are very likely to be pseudobulge-hosting UDGs—a morphological class previously unrecognized in galaxy surveys.

4. CONCLUSION

Our analysis robustly excludes the possibility that pseudobulge-hosting UDGs, exemplified by AGC721966, represent massive galaxies or misclassified nucleated dwarfs with spurious distance measurements. These systems are unambiguously identified as dwarf galaxies (UDGs) harboring pseudobulges.

The absence of both a SMBH and a massive dark matter halo in AGC721966 disfavors the “failed L^* galaxy” hypothesis.

Spectroscopic diagnostics reveal a pronounced α -element enhancement and an ancient stellar population in the pseudobulge. These findings provide robust evidence for the “star-free” merger-driven formation model proposed by Rong et al. (2025), i.e., the pseudobulge emerges from dissipative, gas-rich halo-halo mergers at high redshift, triggering rapid centrally concentrated star formation, while the outer stellar disk results from the recent gas accretion onto the merger remnant, whose elevated spin inherited from the progenitor system’s orbital angular momentum, channels

infalling material into an extended low-surface-brightness disk.

YR acknowledges supports from the NSFC grant 12273037, the CAS Pioneer Hundred Talents Program (Category B), and the USTC Research Funds of the Double First-Class Initiative. HXZ acknowledges support from the NSFC grant

11421303. HYW is supported by the National Natural Science Foundation of China (NSFC, Nos. 12192224) and CAS Project for Young Scientists in Basic Research, Grant No. YSBR-062. This work is supported by the China Manned Space Program with grant no. CMS-CSST-2025-A06 and CMS-CSST-2025-A08.

REFERENCES

- Alam, S., Albareti, F. D., Allende Prieto, C., et al. 2015, *Astrophys. J. Suppl. Ser.*, 219, 12
- Amorisco, N. C., Loeb, A. 2016, *Mon. Not. R. Astron. Soc.*, 459L, 51
- Amorisco, N. C., Monachesi, A., Agnello, A., White, S. D. M. 2018, *Mon. Not. R. Astron. Soc.*, 475, 4235
- Baldwin, J. A., Phillips, M. M., Terlevich, R. 1981, *PASP*, 93, 5
- Beifiori, A., Maraston, C., Thomas, D., Johansson, J. 2011, *A&A*, 531A, 109
- Bekki, K. 2008, *Mon. Not. R. Astron. Soc.: Lett.*, 388, L10
- Bell, E. F., McIntosh, D. H., Katz, N., Weinberg, M. D. 2003, *The Astrophysical Journal Supplement Series*, 149, 289
- Bellazzini, M., Belokurov, V., Magrini, L., Fraternali, F., Testa, V., Beccari, G., Marchetti, A., Carini, R. 2017, *MNRAS*, 467, 3751
- Benavides, J., Sales, L. V., Abadi, M. G., Marinacci, F., Vogelsberger, M., Hernquist, L. 2023, *Monthly Notices of the Royal Astronomical Society*, 522, 1033
- Bidaran, B., Pasquali, A., Lisker, T., Coccato, L., Falcón-Barroso, J., van de Ven, G., Peletier, R., Emsellem, E., Grebel, E. K., La Barbera, F., Janz, J., Sybilska, A., Vijayaraghavan, R., Gallagher, J., III, Gadotti, D. A. 2020, *MNRAS*, 497, 1904
- Burkert, A. 1995, *The Astrophysical Journal*, 447, 25
- Cappellari, M. 2017, *Mon. Not. R. Astron. Soc.*, 466, 798
- Cappellari, M. 2023, *Mon. Not. R. Astron. Soc.*, 526, 3273
- Cardona-Barrero, S., Di Cintio, A., Brook, C. B. A., Ruiz-Lara, T., Beasley, M. A., Falcón-Barroso, J., Maccò, A. V. 2020, *Monthly Notices of the Royal Astronomical Society*, 497, 4282
- Carleton, T., Errani, R., Cooper, M., Kaplinghat, M., Peñarrubia, J., Guo, Y. 2019, *Monthly Notices of the Royal Astronomical Society*, 485, 382
- Chan, T. K., Kereš, D., Wetzel, A., Hopkins, P. F., Faucher-Gigu'ree, C.-A., El-Badry, K., Garrison-Kimmel, S., Boylan-Kolchin, M. 2018, *Monthly Notices of the Royal Astronomical Society*, 478, 906
- Di Cintio, A., Brook, C. B., Dutton, A. A., Maccò, A. V., Obreja, A., Dekel, A. 2016, *Monthly Notices of the Royal Astronomical Society: Letters*, 466, L1
- Dopita, M. A., Kewley, L. J., Sutherland, R. S., Nicholls, D. C. 2016, *Astrophysics and Space Science*, 361, 61
- Drinkwater, M. J., Jones, J. B., Gregg, M. D., Phillipps, S. 2000, *Publications of the Astronomical Society of Australia*, 17, 227
- Emsellem, E., Cappellari, M., Peletier, R. F., McDermid, R. M., Bacon, R., Bureau, M., Copin, Y., Davies, R. L., Krajnović, D., Kuntschner, H., Miller, B. W., de Zeeuw, P. T. 2004, *Mon. Not. R. Astron. Soc.*, 352, 721
- Fahrion, K., Lyubenova, M., van de Ven, G., Leaman, R., Hilker, M., Martín-Navarro, I., Zhu, L., Alfaro-Cuello, M., Coccato, L., Corsini, E. M., Falcón-Barroso, J., Iodice, E., McDermid, R. M., Sarzi, M., de Zeeuw, T. 2019, *Astronomy & Astrophysics*, 628, 92
- Fahrion, K., Gvozdenko, M. A., Beasley, A., Guerra Arencibia, S., Jerabkova, T., Fensch, J., Emsellem, E. 2025, eprint arXiv:2503.03404
- Ferré-Mateu, A., Alabi, A., Forbes, D. A., Romanowsky, A. J., Brodie, J., Pandya, V., Martín-Navarro, I., Bellstedt, S., Wasserman, A., Stone, M. B., Okabe, N. 2018, *Mon. Not. R. Astron. Soc.*, 479, 4891
- Ferré-Mateu, A., Gannon, J. S., Forbes, D. A., Buzzo, M. L., Romanowsky, A. J., Brodie, J. P. 2023, *Mon. Not. R. Astron. Soc.*, 526, 4735
- Fitzpatrick, E. L. 1999, *PASP*, 111, 63
- Gannon, J. S., Forbes, D. A., Romanowsky, A. J., Ferré-Mateu, A., Couch, W. J., Brodie, J. P., Huang, S., Janssens, S. R., Okabe, N. 2022, *Mon. Not. R. Astron. Soc.*, 510, 946
- Gault, L., Leisman, L., Adams, E. A. K., Mancera Pi na, P. E., Reiter, K., Smith, N., Battipaglia, M., Cannon, J. M., Fraternali, F., Haynes, M. P., McAllan, E., Pagel, H. J., Rhode, K. L., Salzer, J. J., Singer, Q. 2021, *ApJ*, 909, 19
- Georgiev, I. Y., Böker, T., Leigh, N., Lützgendorf, N., Neumayer, N. 2016, *Monthly Notices of the Royal Astronomical Society*, 457(2), 2122
- Girelli, G., Pozzetti, L., Bolzonella, M., Giocoli, C., Marulli, F., Baldi, M. 2020, *A&A*, 634A, 135
- Greene, J. E., Seth, A., Kim, M., Läsker, R., Goulding, A., Gao, F., Braatz, J. A., Henkel, C., Condon, J., Lo, K. Y., Zhao, W. 2016, *ApJL*, 826, 32
- Grishin, K. A., Chilingarian, I. V., Afanasiev, A. V., Fabricant, D., Katkov, I. Y., Moran, S., Yagi, M. 2021, *Nature Astronomy*, 5, 1308

- Gu, M., Conroy, C., Law, D., van Dokkum, P., Yan, R., Wake, D., Bundy, K., Merritt, A., Abraham, R., Zhang, J., Bershadsky, M., Bizyaev, D., Brinkmann, J., Drory, N., Grabowski, K., Masters, K., Pan, K., Parejko, J., Weijmans, A. M., Zhang, K. 2018, *ApJ*, 859, 37
- Guérout, A., Krajnović, D., Epinat, B., Contini, T., Emsellem, E., Bouché, N., Bacon, R., Michel-Dansac, L., Richard, J., Weilbacher, P. M., Schaye, J., Marino, R. A., den Brok, M., Erroz-Ferrer, S. 2017, *A&A*, 608A, 5
- Häring, N., Rix, H.-W. 2004, *ApJL*, 604, 89
- Hartke, J., Iodice, E., Gullieuszik, M., Mirabile, M., Buttitta, C., Doll, G., DÁgo, G., de la Casa, C. C., Hess, K. M., Kotulla, R., Poggianti, B., Arnaboldi, M., Cantiello, M., Corsini, E. M., Falcón-Barroso, J., Forbes, D. A., Hilker, M., Mieske, S., Rejkuba, M., Spavone, M., Spinelli, C. 2025, *A&A*, 695A, 71
- Haynes, M. P., Giovanelli, R., Kent, B. R., Adams, E. A. K., Balonek, T. J., Craig, D. W., Fertig, D., Finn, R., Giovanardi, C., Hallenbeck, G., Hess, K. M., Hoffman, G. L., Huang, S., Jones, M. G., Koopmann, R. A., K. A. M., Neira, D. B., Rhode, K. L., R. A. S. et al. 2018, *Astrophys. J.*, 861, 49
- Hilker, M., Infante, L., Vieira, G., Kissler-Patig, M., Richtler, T. 1999, *Astron. Astrophys. Suppl. Ser.*, 134, 75
- Holtzman, J. A., Faber, S. M., Shaya, E. J., Lauer, T. R., Groth, J., Hunter, D. A., Baum, W. A., Ewald, S. P., Hester, J. J., Light, R. M., Lynds, C. R., O’Neil, E. J., Jr., Westphal, J. A. 1992, *AJ*, 103, 691
- Hu, J. 2008, *Mon. Not. R. Astron. Soc.*, 386, 2242
- Hummer, D. G., Storey, P. J. 1987, *MNRAS*, 224, 801
- Izotov, Y. I., Stasińska, G., Meynet, G., Guseva, N. G., Thuan, T. X. 2006, *A&A*, 448, 955
- Jiang, F., Dekel, A., Freundlich, J., Romanowsky, A. J., Dutton, A. A., Macciò, A. V., Di Cintio, A. 2019, *Monthly Notices of the Royal Astronomical Society*, 487, 5272
- Johnston, E. J., Puzia, T. H., DÁgo, G., Eigenthaler, P., Galaz, G., et al. 2020, *Mon. Not. R. Astron. Soc.*, 495, 2247
- Kacharov, N., Neumayer, N., Seth, A. C., Cappellari, M., McDermid, R., Walcher, C. J. 2018, *Mon. Not. R. Astron. Soc.*, 480, 1973
- Kewley, L. J., Dopita, M. A., Sutherland, R. S., Heisler, C. A., Trevena, J. 2001, *The Astrophysical Journal*, 556, 121
- Kewley, L. J., Groves, B., Kauffmann, G., Heckman, T. 2006, *Mon. Not. R. Astron. Soc.*, 372, 961
- Kirby, E. N., Cohen, J. G., Guhathakurta, P., Cheng, L., Bullock, J. S., Gallazzi, A. 2013, *The Astrophysical Journal*, 779, 102
- Khim, D. J., Zaritsky, D., Sandoval Ascencio, L., Cooper, M. C., Donnerstein, R. 2025, eprint arXiv:2502.19465
- Kormendy, J., Bender, R. 2012, *The Astrophysical Journal Supplement Series*, 198, 2
- Kormendy, J., Drory, N., Bender, R., Cornell, M. E. 2010, *The Astrophysical Journal*, 723, 54
- Kormendy, J., Ho, L. C. 2013, *Annual Review of Astronomy and Astrophysics*, 51, 511
- Kovács, O. E., Bogdán, A., Canning, R. E. A. 2019, *The Astrophysical Journal Letters*, 879, 12
- Kniazev, A. Y., Pustilnik, S. A., Grebel, E. K., Lee, H., Pramskij, A. G. 2004, *The Astrophysical Journals*, 153, 429
- Lee, H., Skillman, E. D., Cannon, J. M., Jackson, D. C., Gehrzi, R. D., Polomski, E. F., Woodward, C. E. 2006, *ApJL*, 647L, 970
- Lelli, F., McGaugh, S. S., Schombert, J. M. 2016, *The Astrophysical Journal Letters*, 816, L14
- Liao, S., Gao, L., Frenk, C. S., Grand, R. J. J., Guo, Q., Gómez, F. A., Marinacci, F., Pakmor, Rüdiger, Shao, S., Springel, V. 2019, *Monthly Notices of the Royal Astronomical Society*, 490, 5182
- Lim, S., Côté, P., Peng, E. W., Ferrarese, L., Roediger, J. C., Durrell, P. R., Mihos, J. C., Wang, K., Gwyn, S. D. J., Cuillandre, J.-C., Liu, C., et al. 2020, *The Astrophysical Journal*, 899, 69
- Marleau, F. R., Duc, P.-A., Poulain, M., M’uller, O., Lim, S., Durrell, P. R., Sánchez-Janssen, R., Paudel, S. 2024, *Astronomy & Astrophysics*, 690, 339
- Martín-Navarro, I., Romanowsky, A. J., Brodie, J. P., Ferré-Mateu, A., Alabi, A., Forbes, D. A., Sharina, M., Villaume, A., Pandya, V., Martínez-Delgado, D. 2019, *MNRAS*, 484, 3425
- Neumayer, N., Seth, A., B’oker, T. 2020, *The Astronomy and Astrophysics Review*, 28, 4
- Nguyen, D. D., Seth, A. C., den Brok, M., Neumayer, N., Cappellari, M., Barth, A. J., Caldwell, N., Williams, B. F., Binder, B. 2017, *ApJ*, 836, 237
- O’Connell, R. W., Gallagher, J. S., Hunter, D. A., Colley, W. N. 1995, *The Astrophysical Journal*, 446L, 1
- Pettini, M., Pagel, B. E. J. 2004, *Mon. Not. R. Astron. Soc.*, 348, L59
- Pietrinferni, A., Cassisi, S., Salaris, M., Castelli, F. 2006, *The Astrophysical Journal*, 642, 797
- Rong, Y., Guo, Q., Gao, L., Liao, S., Xie, L., Puzia, T. H., Sun, S., Pan, J. 2017, *Monthly Notices of the Royal Astronomical Society*, 470, 4231
- Rong, Y., Zhu, K., Johnston, E. J., Zhang, H.-X., Cao, T., Puzia, T. H., Galaz, G. 2020, *The Astrophysical Journal Letters*, 899, 12
- Rong, Y., Mancera Pi na, P. E., Tempel, E., Puzia, T. H., De Rijcke, S. 2020, *Monthly Notices of the Royal Astronomical Society: Letters*, 498, L72
- Rong, Y., Huijie, H., Min, H., Wei, D., Qi, G., Hui-Yuan, W., Hong-Xin, Z. 2024, arXiv e-prints:2404.00555
- Rong, Y., Zhang, H., Cheng, C., et al. 2025, *The Astrophysical Journal Letters*, 978, 44
- Salucci, P., Lapi, A., Tonini, C., Gentile, G., Yegorova, I., Klein, U. 2007, *Mon. Not. R. Astron. Soc.*, 378, 41
- Schutte, Z., Reines, A. E., Greene, J. E. 2019, *The Astrophysical Journal*, 887, 245

- Seth, A. C., Blum, R. D., Bastian, N., Caldwell, N., Debattista, V. P. 2008, *The Astrophysical Journal*, 687, 997
- Sifón, C., van der Burg, R. F. J., Hoekstra, H., Muzzin, A., Herbonnet, R. 2018, *Mon. Not. R. Astron. Soc.*, 473, 3747
- Spengler, C., Côté, P., Roediger, J., Ferrarese, L., Sánchez-Janssen, R., Toloba, E., Liu, Y., Guhathakurta, P., Cuillandre, J.-C., et al. 2017, *The Astrophysical Journal*, 849(1), 55
- Spinello, C., Tortora, C., DÁgo, G., Coccato, L., La Barbera, F., Ferré-Mateu, A., Pulsoni, C., Arnaboldi, M., Gallazzi, A., Hunt, L., Napolitano, N. R., Radovich, M., Scognamiglio, D., Spavone, M., Zibetti, S. 2021, *A&A*, 654A, 136
- Stark, D. V., McGaugh, S. S., Swaters, R. A. 2009, *The Astronomical Journal*, 138, 392
- Tremaine, S., Gebhardt, K., Bender, R., Bower, G., Dressler, A., Faber, S. M., Filippenko, A. V., Green, R., Grillmair, C., Ho, L. C., et al. 2002, *The Astrophysical Journal*, 574, 740
- Trujillo, I., Roman, J., Filho, M., Sánchez Almeida, J. 2017, *The Astrophysical Journal*, 836, 191
- Valdes, F., Gupta, R., Rose, J. A., Singh, H. P., Bell, D. J. 2004, *ApJS*, 152, 251
- van Dokkum, P., Abraham, R., Merritt, A., Zhang, J., Geha, M. 2015, *Astrophys. J. Letters*, 798, L45
- van Dokkum, P., Abraham, R., Brodie, J., Conroy, C., Danieli, S., Merritt, A., Mowla, L., Romanowsky, A. J., Zhang, J. 2016, *Astrophys. J. Letters*, 828, 6
- van Dokkum, P. 2018, *Nature*, 555, 629
- van Dokkum, P., Danieli, S., Abraham, R., Conroy, C., Romanowsky, A. J. 2019, *The Astrophysical Journal Letters*, 874, L5
- Vazdekis, A., Coelho, P., Cassisi, S., Ricciardelli, E., Falcón-Barroso, J., Sánchez-Blázquez, P., La Barbera, F., Beasley, M. A., Pietrinferni, A. 2015, *Mon. Not. R. Astron. Soc.*, 449, 1177
- Walcher, C. J., Böker, T., Charlot, S., Ho, L. C., Rix, H.-W., Rossa, J., Shields, J. C., van der Marel, R. P. 2006, *The Astrophysical Journal*, 649, 692
- Wang, J., Koribalski, B. S., Serra, P., van der Hulst, T., Roychowdhury, S., Kamphuis, P., Chengalur, J. N. 2016, *Mon. Not. R. Astron. Soc.*, 460, 2143
- Wang, J., Bose, S., Frenk, C. S., Gao, L., Jenkins, A., Springel, V., White, S. D. M. 2020, *Nature*, 585, 39
- Whitmore, B. C., Zhang, Q., Leitherer, C., Fall, S. M., Schweizer, F., Miller, B. W. 1999, *AJ*, 118, 1551
- Wright, Anna C., et al. 2021, *Mon. Not. R. Astron. Soc.*, 502, 5370
- Yozin, C., Bekki, K. 2015, *Mon. Not. R. Astron. Soc.*, 452, 937
- Zhang, Z., Chen, Y., Rong, Y., Wang, H., Mo, H., Luo, X., Li, H. 2025, *Nature accepted, arXiv e-prints:2406.10329*